Science of the Total Environment 793 (2021) 148649

Contents lists available at ScienceDirect

Science of the Total Environment

journal homepage: www.elsevier.com/locate/scitotenv

3D dynamic model empowering the knowledge of the decontamination mechanisms and controlling the complex remediation strategy of a contaminated industrial site

Paolo Ciampi [a,*], Carlo Esposito [a], Ernst Bartsch [b], Eduard J. Alesi [b], Marco Petrangeli Papini [c]

[a] Department of Earth Sciences, Sapienza University of Rome, Piazzale Aldo Moro 5, 00185 Rome, Italy
[b] IEG Technologie GmbH, Hohlbachweg 2, D-73344 Gruibingen, Baden-Württemberg, Germany
[c] Department of Chemistry, Sapienza University of Rome, Piazzale Aldo Moro 5, 00185 Rome, Italy

HIGHLIGHTS

- 3D hydrogeochemical model governs all phases of remediation strategy over time.
- Multi-source model reveals decontamination mechanisms due to remediation actions.
- Groundwater circulation wells and a system of electron donor boost bioremediation.
- Multi-temporal imaging unmasks hydraulic influences and biological processes.
- Time trend volume of chlorinated solvent plume quantifies the technique efficacy.

GRAPHICAL ABSTRACT

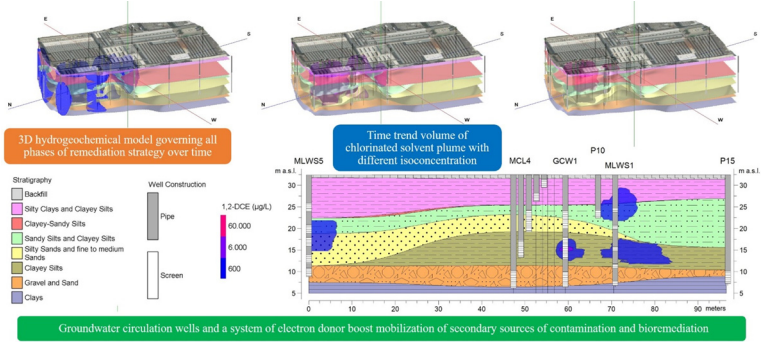

ARTICLE INFO

Article history:
Received 11 April 2021
Received in revised form 4 June 2021
Accepted 20 June 2021
Available online 24 June 2021

Editor: Frederic Coulon

Keywords:
Hydrogeochemical model
Geodatabase
Groundwater circulation well
In situ bioremediation
Secondary contamination source
Biological reductive dechlorination

ABSTRACT

Knowledge of the geology and hydrogeology of the polluted site emblematize a key requirement for environmental remediation, through assembling and synthesizing findings from various sources of physical evidence. In an increasingly virtual era, digital and geo-referenced metadata may serve as tools for collecting, merging, matching, and understanding multi-source information. The main goal of this paper is to emphasize the significance of a 3D hydrogeochemical model to the portrayal and the understanding of contamination dynamics and decontamination mechanisms at a highly contaminated industrial site. Some remediation measures are active on-site, due to the evidence-based presence of chlorinated solvents in groundwater. These are attributable to a slow-release source of pollutants in the saturated zone associated with very low permeability sediments. Therefore, in this research, a new technique for the remediation of secondary sources of dense non-aqueous phase liquid (DNAPL) contamination was investigated for the first time on a full-scale application. The combination of groundwater circulation wells (IEG-GCW®) and a continuous electron donor production device was set up to boost in situ bioremediation (ISB). A multi-phase approach was followed handling and releasing data during various remediation stages, from site characterization via pilot testing to full-scale remediation, thus allowing users to monitor, analyze, and manipulate information in 3D space-time. Multi-source and multi-temporal scenarios reveal the impact of ongoing hydraulic dynamics and depict the decontamination mechanisms in response to the interventions implemented over time, by quantifying the overall performance of the adopted strategies in terms of removal of secondary sources of pollution still active at the site.
© 2021 The Authors. Published by Elsevier B.V. This is an open access article under the CC BY-NC-ND license (http://creativecommons.org/licenses/by-nc-nd/4.0/).

* Corresponding author.
E-mail addresses: paolo.ciampi@uniroma1.it (P. Ciampi), carlo.esposito@uniroma1.it (C. Esposito), ernst.bartsch@ieg-technology.com (E. Bartsch), eduard.alesi@ieg-technology.com (E.J. Alesi), marco.petrangelipapini@uniroma1.it (M. Petrangeli Papini).

https://doi.org/10.1016/j.scitotenv.2021.148649
0048-9697/© 2021 The Authors. Published by Elsevier B.V. This is an open access article under the CC BY-NC-ND license (http://creativecommons.org/licenses/by-nc-nd/4.0/).

1. Introduction

1.1. An overview of chlorinated solvent contamination scenarios

In industrial activities requiring material cleaning or routine ordinary maintenance of mechanical components, chlorinated solvents have been extensively employed since the 1950s (Ebrahimbabaie and Pichtel, 2021; Filippini et al., 2018). The most common and used chlorinated solvents are certainly tetrachloroethylene (PCE) and trichloroethylene (TCE) (Walaszek et al., 2021). These substances represent the category of pollutants most frequently detected in groundwater contamination phenomena because of their extensive application and their peculiar chemical-physical properties, such that they are often found in groundwater in the form of an 'anthropogenic' background (Azzellino et al., 2019). They are liquids that are essentially water-immiscible due to their limited solubility. Organohalogen compounds are also significantly denser than water. For this reason, when they are not fully dissolved, they behave as a so-called DNAPL (Dense Non-Aqueous Phase Liquid), a non-aqueous liquid phase that is denser than water (Ebrahimbabaie and Pichtel, 2021). The latter constitutes a separate phase from the water and tends to stratify below the water table due to its higher density. DNAPLs infiltrate the subsurface as a separate phase following primary contamination events and migrate downwards, by gravity, to saturated portions of the soil (Engelmann et al., 2019). A fraction of the contaminant (defined as the residual fraction) remains trapped in its pathway in the porosity of the soil, retained by forces of physical nature (essentially for capillarity) strictly dependent on the particle size of the crossed medium (Nsir et al., 2018). In the subsurface, DNAPL redistributes to its particular conformation, also known as DNAPL architecture (Carey et al., 2014; Mackay et al., 1985; Newell et al., 2006). In the definition of conceptual models of chlorinated solvent pollution, this redistribution represents the big unknown. Once redistributed, DNAPL persists in an 'immobile' form in the subsurface for a time that relies primarily on the site's peculiarities (Day-Lewis et al., 2017). This DNAPL thus behaves as a persistent source of pollution by releasing components steadily and slowly through the unsaturated part and into the subsurface saturated portion (Koch and Nowak, 2015). The understanding of DNAPL behavior in contamination events and the identification of the best approaches to remediation has been consolidated after more than 30 years of research and field experience (Brooks et al., 2021; Brusseau and Guo, 2014; Colombano et al., 2021; Douglas et al., 2017). Starting from very simplified preliminary models (Mackay et al., 1985), the current definition of a 'life cycle' (Carey et al., 2014) of a chlorinated solvent contamination source, characterized by specific stages of so-called aging, has been achieved. This follows via five aging stages that begin with the primary event of contamination and terminate with complete separate phase depletion (DNAPL). The aquifer contamination persists due to so-called back diffusion and desorption phenomena from low permeability layers (Yang et al., 2018). As a whole, depending on the amount of solvents spilled and the hydrogeological characteristics of the site, these phases could extend from many decades to many hundreds of years (Carey et al., 2014; Heron et al., 2016; Newell et al., 2006). The aging stage then defines the relative distribution of residual solvent mass among environmental matrices (Yang et al., 2018). Identifying the aging status of a given site is essential both to select the most appropriate remediation intervention and to understand and interpret the dynamics of contamination and their dependence on the remediation actions that are implemented over the years (Kueper et al., 2014).

1.2. The biological reductive dechlorination process

Moreover, some chlorinated solvents are subject to natural biodegradation phenomena (biological reductive dechlorination, BRD) that usually, in contaminated sites, are limited by the lack of electron donors (Aulenta et al., 2007a). BRD of chlorinated solvents occurs under optimal redox conditions, through the progressive replacement of chlorine atoms present on the molecule with hydrogen atoms under anaerobic conditions (Aulenta et al., 2007b). Consequently, the higher chlorinated molecules (PCE and TCE) gradually lose their chlorine atoms, generating products with a lower degree of chlorination, such as 1,2-dichloroethylene (1,2-DCE) and vinyl chloride (VC), until the formation of simple and non-toxic aliphatic hydrocarbons such as ethane and ethylene (Aulenta et al., 2007a; Aulenta et al., 2007b; Ebrahimbabaie and Pichtel, 2021; Walaszek et al., 2021). BRD technology usually consists of groundwater injection of readily fermentable substrates that can supply electron donors and thus stimulate the potentially present biological reducing activity (Borden et al., 2019; Davis and Miller, 2018; Lee et al., 2007). Some studies observe an accumulation of toxic compounds with a low chlorination grade (i.e., 1,2-DCE and VC) due to a lack of electron donors (essential elements for biodegradation) (Mayer-Blackwell et al., 2017; Sleep et al., 2005; Yu et al., 2018). Also, lower chlorinated compounds can be recalcitrant to biodegradation due to lack of appropriate microorganisms (anaerobic dechlorinators), unfavorable redox conditions, thermo-kinetic limitations, and a decrease in the number of chlorine substituents during the sequential process of BRD (Stroo and Ward, 2010; Tiehm and Schmidt, 2011). It is important to reiterate how this conceptual framework, which identifies the dynamics and transformations of sources of DNAPL contamination, has been consolidated only in recent years and, consequently, has paved the way for the development of remediation technologies and strategies that were previously not known or considered impractical.

1.3. The Groundwater Circulation Well (IEG-GCW®) technology

This is the background for innovative remediation technologies such as Groundwater Circulation Wells (IEG-GCW®). A vertical pressure gradient between two or more hydraulically separated sections of a well may be developed by IEG-GCW®s, inducing the formation of circulation cells in the aquifer (Dinkel et al., 2020; Herrling et al., 1991a, 1991b; Johnson and Simon, 2007; Xia et al., 2019; Zhu et al., 2020). In practice, groundwater is extracted through a fenestrated fragment of a multi-fenestrated well, moves through a treatment unit, and is then reinjected through a different fenestrated segment directly into the aquifer body (Herrling et al., 1991a, 1991b). The vertical component of the flow triggered by recirculation effectively intercepts portions of the aquifer potentially impacted by the accumulation of contaminants and not reachable with traditional pumping systems (Tatti et al., 2019). The recirculation pattern is adapted based on the chemical/physical characteristics of the pollutants and the lithostratigraphic peculiarities of the site, favoring the flow through the zones with lower permeability, the mobilization of adsorbed contaminants, and significantly improving the aquifer's remediation capacity (Pierro et al., 2017). Recirculation with the IEG-GCW® system induces a drastic acceleration of contaminant mobilization processes compared to a conventional Pump&Treat (P&T), significantly increasing the amount of mass removed per unit of time (Petrangeli Papini et al., 2016). Besides that, the process does not produce wastewater, but the treated water is recirculated within the same aquifer. The patented treatment device considered in this research consists of a poly-3-hydroxybutyrate (PHB) containing reactor for the persistent output of electron donors and a zero-valent iron-containing reactor (Matturro et al., 2018; Petrangeli Papini et al., 2016; Pierro et al., 2017). Zero-valent iron (ZVI/Fe) is a well-known reactive material commonly used to dechlorinate chlorinated solvents with abiotic reduction (Ebrahimbabaie and Pichtel, 2021; Liu et al., 2006; Tseng et al., 2011). This groundbreaking technology aspires to enhance biological reductive dechlorination in situ by combining groundwater circulation wells with a continuous electron donor production process (Petrangeli Papini et al., 2016).

1.4. Multi-source data fusion supporting the remediation strategy

The aforementioned concepts reveal that the symbiosis of all the information usually accessible at polluted sites, the assembly and

synthesis of contributions from multiple lines of chemical-physical evidence (Orozco et al., 2021) are crucial prerequisites for environmental remediation (Ciampi et al., 2019a; Cormier and Suter, 2008; Kueper et al., 2014). In this sense, this research pursues the centralization and the overlapping of knowledge inherent to the geological, hydrochemical, and engineering realities into a single digital Conceptual Site Model (Ciampi et al., 2019b). Hence, the perspective to predispose actions with remediation technologies unequivocally adapted and adjusted to the site-specific peculiarities and to the real features of the contaminant, which is inserted in the unique hydrogeological architecture, might be unlocked (Ciampi et al., 2021). The above can boost each discipline's contribution to the growth of a single progressive workflow. The fusion of all the components involved in environmental remediation and of multiple forms of geomodeling into a geo-referenced framework may serve as a tool for handling, combining, linking, and interpreting multi-source data (Breunig et al., 2020; Ciampi et al., 2019a). The goal of this research would be to demonstrate the contribution of a 3D hydrogeochemical clone to the refinement of the conceptual site model, to the lecture of contamination/decontamination dynamics, and the interpretation of the effects arising from the adoption of reclamation techniques at a highly contaminated industrial site. Such is the case of an engineering factory located in an industrial district in the Po Valley and characterized by a complex geological architecture. Until 1987, the plant, which is still operational, housed washing machines using chlorinated solvents for degreasing mechanical parts. Some strategies to characterize and remediate the site have been undertaken over time in the industrial plant, due to the evidence-based presence of chlorinated solvents in groundwater. High-resolution hydrochemical characterization identified a large mass of pollutants in correspondence with fine material lenses, representing a slow-release source of pollutants in the saturated zone with very low permeability (Ciampi et al., 2019b). For the first time on a full scale, IEG-GCW®s coupled with in situ bioremediation (ISB) (Matturro et al., 2018; Pierro et al., 2017) are being applied and evaluated. Such a novel dual technology may constitute a powerful option for integrating, accelerating, and enhancing the pollutant removal efforts of the remediation activities already onsite, by targeting directly the secondary sources of active contamination. In this challenging and cross-disciplinary scenario, 3D hydrochemical models could potentially depict and quantify the effect of the applied remediation approach (Ouyang et al., 2017) on the abatement of pollutants and the mitigation of secondary contamination sources still active at the site. Multi-source and multi-phase pictures reveal the impact of ongoing hydraulic dynamics and depict the decontamination mechanisms in relation to the application and modification of remediation actions over time, quantifying the performance of the adopted strategies.

2. Materials and methods

2.1. History of site characterization and remediation

Some actions aimed at characterizing and remediating the site have been undertaken over time (from 2001 to 2017) in the industrial plant, following the proven occurrence of chlorinated aliphatic compounds in the groundwater. Characterization and in-depth investigations had as purpose to furnish technical knowledge for the identification and management of the appropriate remediation methods to gradually reduce the ascertained forms of contamination (Dai et al., 2018; Langwaldt and Puhakka, 2000). A preliminary investigation in 2001 suggested designing a piezometric monitoring network and a system of pumping wells within the site and a hydraulic barrier on the northwest perimeter of the plant. Supplemental surveys in 2012 supported the installation of multi-level piezometers (IEG-MLWS®) (following the example of Puigserver et al., 2020), the planning of a distributed control system (DCS) (Arlotti et al., 2012), and the pilot-scale setup of the groundwater circulation well (IEG-GCW®) at the recognized secondary contamination source (Ciampi et al., 2019b; Petrangeli Papini et al., 2016; Pierro et al., 2017). Cluster (CL) and multi-cluster (MCL) piezometers, which are equipped with 2 and 5 filtered sections, respectively, for vertical sampling, were installed during the same period (similarly to the case of Moeck et al., 2017). Supplemental studies dating back to 2017 were planned to locate two additional IEG-GCW®s and further MLWSs in the center of the plant, around the building that housed industrial washing machines, which constituted the primary sources of contamination. Four remediation steps are distinguishable based on the undertaken actions. The first phase, which lasted until 2013, entails groundwater extraction through traditional pumping and barrier wells and hydrochemical monitoring of the piezometric network. The second remediation step deals with the first GCW implementation at the pilot scale (GCW1) in 2014. Full-scale strategy deployment follows in 2019, through the realization of two further GCWs (GCW2 and GCW3). The last remediation phase, corresponding to 2020, foresees the remodulation and reduction of the flow rates of the pumping wells inside the plant.

2.2. The hydrogeochemical geodatabase

Information obtained from both characterization and monitoring plans was stored in a geodatabase (Ciampi et al., 2019a). The latter is a digital archive of structured and geo-referenced data, containing knowledge related to the different scientific spheres, which were gathered from surveys and field investigations covering a surface of 120,000 m^2. Relational and four-dimensional (4D) databases (Ciampi et al., 2021) encourage the joint management and fusion of multi-source data by optimizing time-series analysis of parameters (Ciampi et al., 2019a). The data management framework contains the geological features of the study site, which were deduced from 56 drilled boreholes, reaching a maximum depth of approximately 30 m. Also, the pumping rates of extraction wells, the hydrochemical data, the construction sketches, and configuration related to wells, piezometers (i.e., screened and blind portions), and remediation plant are included in the geodatabase. The installation of numerous piezometers and wells over the years has encouraged an increase in the number of groundwater monitoring points over time. This rose from 53 points in 2013, through 68 in 2014, to 106 points in the 2020 monitoring network. The different configuration of network points has as goal to guarantee groundwater sampling at multiple depth intervals. The definition, monitoring, and reconfiguration of the intervention technique were optimized based on an examination of the vast amount of chemical characterization analyses available on the entire monitoring network since 2008.

2.3. The multitemporal modeling process

The interpolation and modeling activities carried out on the geological-chemical data aspire to reconstruct the hydrogeological architecture of the subsoil within the plant and to provide insight into the quality status of groundwater (Ciampi et al., 2021). Interpolation of piezometric measurements intends to delineate the groundwater flow pattern. RockWorks 17 was adopted for spatial analysis operations (Ciampi et al., 2019a; Ciampi et al., 2019b). Inverse distance weighting (IDW) was employed as the algorithm to interpolate geological and hydrochemical variables in the domain of a 3D mesh consisting of voxels (Barbosa et al., 2019; Trabelsi et al., 2013; Zhu et al., 2013). The mesh of the 3D model covers the facility area and extends vertically from 1.8 m to 33.4 m above sea level. The voxel grid discretization is 2.0 m in the X, Y directions and 0.2 m in the Z direction. The goal is to demonstrate the consequences of IEG-GCW®-induced recirculation and pumping activities on the dynamics and mechanisms of the decontamination process. Integrative surveys cluster (CL and MCL) and MLWS piezometers distributed around the IEG-GCW®s were designed to strengthen the conceptual model of the plant area in which the interventions are embedded, by capturing a high-resolution characterization of subsurface geological heterogeneity (Orozco et al., 2021) and vertical

zonation of contamination (Steelman et al., 2020). The goal of this was, on the one hand, to adapt the design of IEG-GCW® and DCS to site-specific geological peculiarities and, on the other hand, to furnish the necessary knowledge for assessing the performance of the undertaken measures in terms of chlorinated solvent removal from groundwater. To fully understand the evolution of groundwater pollution status and to evaluate the impact of the adopted strategies, 3D solid models depicting the concentration of index chemicals as a function of time have been built from hydrochemical records. Contaminant concentrations detected in the aquifer are portrayed as isosurfaces within the georeferenced 3D space following the approach of Curtis et al. (2019) and Ouyang et al. (2017). The isosurface represents the locus of points in space where a given quantity has the same value (Litvinenko et al., 2020). Through isosurfaces, it is possible to define and isolate a volume of groundwater that is marked by a certain concentration of pollutants. The isosurfaces were generated by interpolation of the concentration values for the different groundwater sampling. Each isoconcentration model expects to deliver a graphical representation and a quantitative calculation of 1,2-dichloroethylene (1,2-DCE) and vinyl chloride (VC) concentration levels detected over time in the piezometric network. The contamination models cover a reference period that takes into account the monitoring campaigns carried out in 2013 (monitoring), 2014 (pilot test), 2019 (full-scale), and 2020 (pumping configuration modification), corresponding to various stages of remediation. The above aims at providing an evolving picture over time and the most up-to-date snapshot of the distribution of solvent concentrations in space, offering the opportunity to assess the impact of the applied remediation strategy for the progressive mitigation of pollution sources still active at the site. The computation of the volumes enclosed inside each isosurface at a different concentration level was extrapolated by post-processing operations on 3D solid models. From the hydrogeochemical model, which superimposes the depiction of the contamination condition on the geologic schemes, profiles were extrapolated close to the primary pollution event and at the first IEG-GCW® installed at the site. A study of the time trend volumes at different isoconcentration of chlorinated solvents and multi-temporal photography of hydrogeochemical scenarios was performed to supply new insights on the abatement capacity of contaminants, in relation to the adoption of multiple remediation actions, and the dynamics of decontamination at the site, directly influenced by hydraulic processes that develop within such a specific geological context. This multi-source, multi-data temporal imaging is intended to unmask the dynamic geochemical and biological interactions that grow and develop following the implementation of a novel intervention strategy, and at the same time, to check and quantify the efficacy of the adopted technique, by estimating the mass balance.

2.4. Geological framework and hydraulic context

The industrial plant is housed inside the geological background marked by sediments of fluvial origin, conoid, and alluvial deposits of the Po Plain, in northern Italy (Guerra et al., 2020). Over the years, on-site investigations have revealed a very complex geological and hydrogeological environment, characterized by a lenticular stratigraphic system, which depicts a pronounced vertical and horizontal heterogeneity of the lithology (Ciampi et al., 2019b). In general, the following levels can be recognized in the subsoil of the plant, in stratigraphic succession from top to bottom:

- Backfill to a depth of 1–1.5 m;
- Silty clays and clayey silts, gray in color, relatively compact, often with peat, bricks, and plant residues, around 8.5 m thick on average;
- Clayey-sandy silts, sandy silts, and clayey silts, with rising downward sandy fraction and varying thickness. This stratum is generally found at a depth between 9 and 12 m;
- Silty sands and fine to medium sands, characterized by an average thickness of 4 m and demarcated by good permeability values, often in continuity with the underlying gravel layer, often isolated by a low permeability lens, were found;
- A discontinuous layer of clayey silts, represented by fine-textured soils that are interposed between the more permeable layers. This layer consists of silts and clayey silts with very low to no permeability and is located at depths between 16.5 m and 20.5 m;
- A stratum, with an average thickness of 4 m, marked by discrete permeability values and guaranteed lateral continuity (gravel and sand);
- An impermeable silty clayey horizon (clays) at a depth of about 25 m from the ground surface, characterized by assured lateral continuity (Ciampi et al., 2019b).

The subsurface lithostratigraphic structure between approximately 9 m and 20.5 m depth is distinguished by a pronounced lateral discontinuity due to the presence of multiple soil lenses of varying textures and permeability. Such lithological variations reflect on the modalities of the underground water circulation, which results to be fractionated in aquifer levels with different permeability, variously communicating among them (Maples et al., 2019). The only aquifer with continuity is the one hosted in the layer of permeable gravels and sands, with a thickness of about 4 m and located at a depth of about 20 m from the ground level. The presence of consistent very low permeability layers, at both the surface and depth, determines the confinement of this aquifer layer. Concerning the groundwater dynamics, it is useful to examine how, on average, the subjacency measured in the piezometers in the area under investigation is equal to 2 m from ground level. The subjacency values display a certain variability in piezometers placed at short distances from each other. The occurrence of piezometric anomalies and strong lateral permeability differences are justified by the complexities of the geological scenario, which is marked by substantial lateral variations in the geometry of the sedimentary bodies and, thus, in the level of the aquifer. The presence of active wells inside the factory, with varying configurations, screened sections in different aquifers, and operating patterns, is another disturbing factor that may clarify the non-homogeneous variations in piezometric levels (Zume and Tarhule, 2008). Certainly, the boundary hydraulic barrier, DCS system, pumping wells, and IEG-GCW®s are the elements that exert the greatest stress on the circulation of groundwater (Fig. 1).

The alternation of sandy or sandy-gravelly layers and clayey-silty horizons results in the fragmentation of the water circulation into multiple levels. The construction of a large number of wells in the area may have connected the aquifer levels where the low permeability layers isolated them (Mayo, 2010; Wu et al., 2015). At the site scale, the isopiezic map illustrates hydrological features. The prevailing direction of the groundwater flow is oriented from the southern to the northern quadrants. The result reveals the strong influence of the boundary hydraulic barrier and internal pumping wells on the groundwater level since the piezometric survey was conducted with the barrier and pumping wells in operation (Zume and Tarhule, 2008). In fact, at the withdrawal points, the pumping wells cause a drawdown of the water table and a pullback of groundwater to the site's NW side (Fig. 2).

However, certain factors that impact piezometry at the site-specific level must be taken into consideration when examining piezometric patterns. At the local level, depending on groundwater dynamics, the existence of a fractured geological architecture, and pumping wells, the flow vectors may diverge more or less from the prevailing direction, which could alter the static dynamics of groundwater flow.

3. Results

3.1. Contamination scenarios and decontamination dynamics

Previous studies revealed that compounds with a high number of chlorine atoms have undoubtedly been employed as industrial solvents

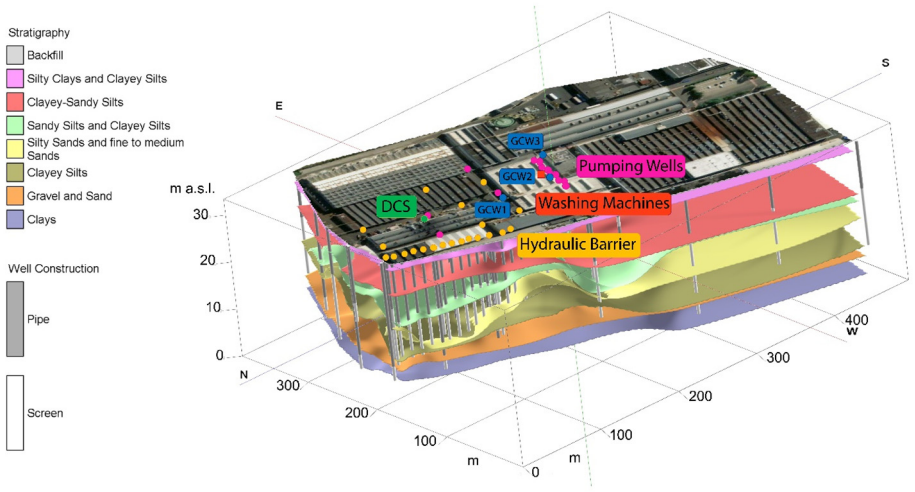

Fig. 1. 3D industrial plant geological model that reflects the complex architecture of the stratigraphic horizons. With the stratigraphic model, the position and construction drawings of wells and piezometers present at the site are combined, showing the operative configuration.

in the past. Uncontrolled spills of these substances led to primary contamination events. Such compounds have been found at considerably lower concentrations than DCE and VC (Fig. 1 of Supplementary Material), demonstrating a significant biological dechlorination activity. Thus DCE and VC constitute BRD's daughter products (Aulenta et al., 2002; Aulenta et al., 2005; Ciampi et al., 2019b; Petrangeli Papini et al., 2016; Pierro et al., 2017). Monitoring data related to 1,2-DCE were used to generate isoconcentration models, differentiated by contamination levels. The 3D plumes depict the evolution of the groundwater pollution status over time and are embedded within the stratigraphic framework of the site. The models identify the portions of the plant affected by the presence of the highest concentrations of 1,2-DCE around the DCS well, at the

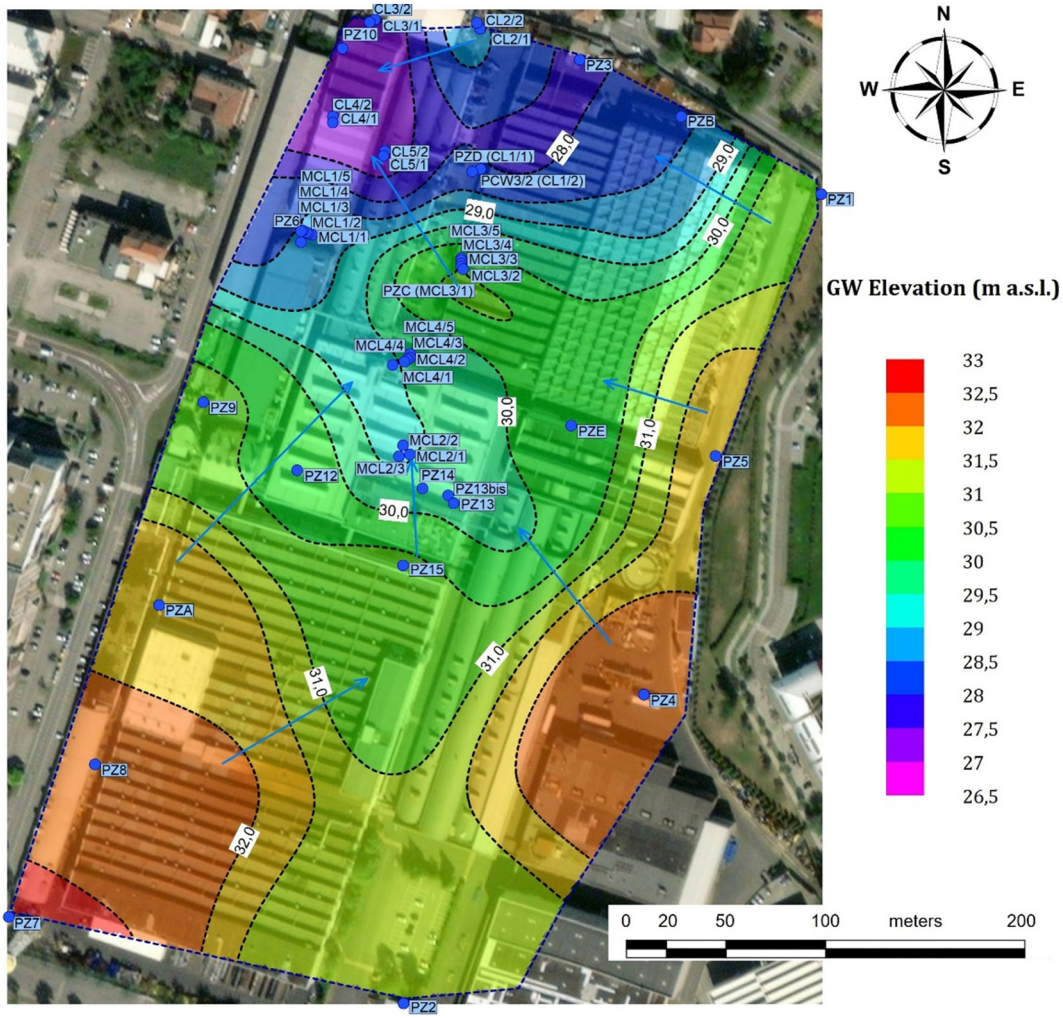

Fig. 2. Isopiezic chart of groundwater elevation measured in the monitoring network. Flow vectors reveal the direction of the local groundwater flow.

peripheral wells of the hydraulic barrier, and below the building that housed industrial washing machines, where the primary contamination event occurred and where IEG-GCW®s were placed. Figs. 3 and 4 illustrate the spatial distribution of contaminants in groundwater in 2013, 2014, 2019, and 2020.

Through the 3D models, the most critical areas can be easily identified, evaluating the trend of pollutant concentrations in the site in relation to the application of remediation actions over time. Multi-temporal photographs present a general overview of the contamination distribution that is particularly inhomogeneous. However, such sketches recognize some well-demarcated areas within the plant in which "active" secondary sources of contamination should be present (Ciampi et al., 2019b; Petrangeli Papini et al., 2016). The portions of the site impacted by significant pollutant concentrations are located in correspondence with the building situated in the center of the plant (the primary contamination source), at the DCS well, and close to the boundary barrier wells. The temporal behaviors observed in most of the examined piezometers exhibit initial higher contaminant concentrations with a progressive and continuous decrease reasonably attributable to the various extraction and recirculation systems that have been gradually deployed over the years (Fig. 1 of Supplementary Material). The volumetric isoconcentration models of 1,2-DCE evidence, especially in the last two years of monitoring, a contraction of the areas impacted by contamination and a decrease, in absolute value, of the amount of dissolved contaminants in groundwater. Moreover, the integrated models associate the significant presence of contaminants to the most shallow and fine layers, characterized by a low permeability, which could act as secondary sources of contamination with a slow release of pollutants (Petrangeli Papini et al., 2016; Pierro et al., 2017). While a substantial reduction in concentration is recorded by several monitoring piezometers, even by several orders of magnitude compared to the initial condition, in some sectors of the plant the concentrations still tend to

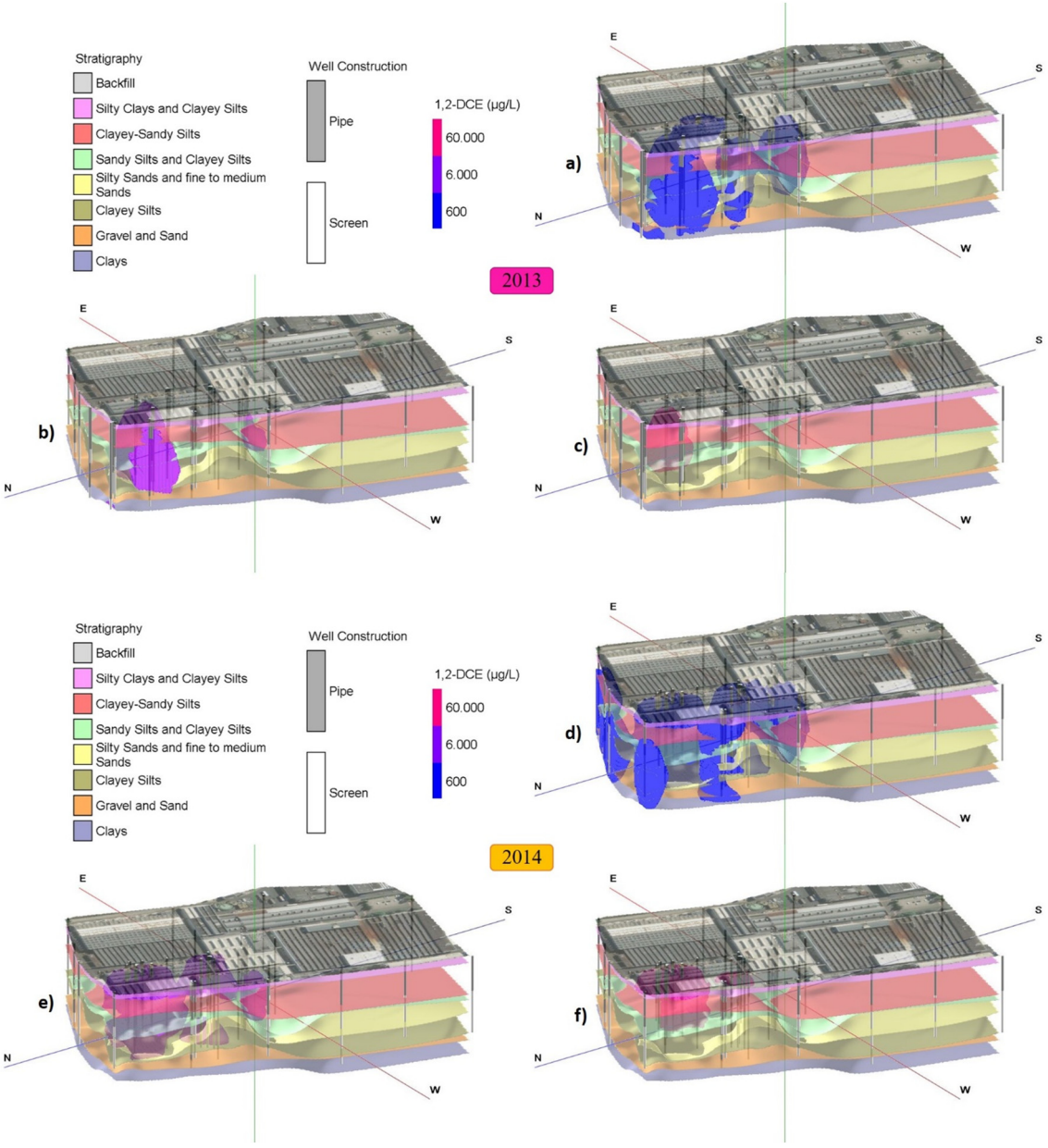

Fig. 3. Stratigraphic contacts, construction scheme of piezometers, and contamination plume at different concentrations of 1,2-DCE detected in the monitoring network in 2013 and 2014. Figures a, b, and c refer to isoconcentration isosurfaces of 600 µg/L, 6000 µg/L, and 60,000 µg/L, respectively detected in 2013. Figures d, e, and f are related to isoconcentration isosurfaces of 600 µg/L, 6000 µg/L, and 60,000 µg/L respectively measured in 2014.

stabilize around values that are still relevant and indicate the presence of slow-release sources governed by back diffusion phenomena (Fig. 1 of Supplementary Material) (Tatti et al., 2019; Ciampi et al., 2019b).

To understand the site-specific decontamination dynamics, it is interesting to focus on two distinct portions of the site. In the central area of the plant, where IEG-GCW®s and some pumping wells are installed (the primary source of contamination), plume models at different concentrations reveal the mobilization of contaminants induced by the recirculating hydraulic systems. Local increases in trends of 1,2-DCE and VC concentrations appear to follow the development of pilot testing (2014), full-scale (2019), and change in pumping configuration (2020) (Fig. 1 of Supplementary Material). Indeed, the confrontation between the images rendered by the set of Fig. 3a, b and c (2013) and that of Fig. 3d, e and f (2014) reveals an expansion of 1,2-DCE plume volumes in the central sector of the plant in 2014, when the pilot test was launched, with respect to 2013. Observation of photographs for 2019 (Fig. 4b) and 2020 (Fig. 4e) evinces the apparition of a 1,2-DCE contamination plume with an isoconcentration of 6000 μg/L, absent in 2019, below the building that contained the industrial washing machines, in the last available monitoring campaign. This effect could be related to the application of full-scale IEG-GCW®s combined with the reduction in the pumping rate of some wells, which were potentially exerting hydraulic disturbance on groundwater recirculation systems in that area. This latter aspect suggests that interference of recirculation cells induced by IEG-GCW®s with the drawdown cone resulting from extraction may play a key role in the mobilization of residual-phase contaminants. All these statements are validated by the hydrogeochemical section extracted from the multi-temporal solid models and located at the source zone. Fig. 5 illustrates the evolving picture of contamination status in the primary source area.

Installation of the first IEG-GCW® at the pilot scale in 2014 induces pollutant mobilization and the 1,2-DCE dissolution in groundwater.

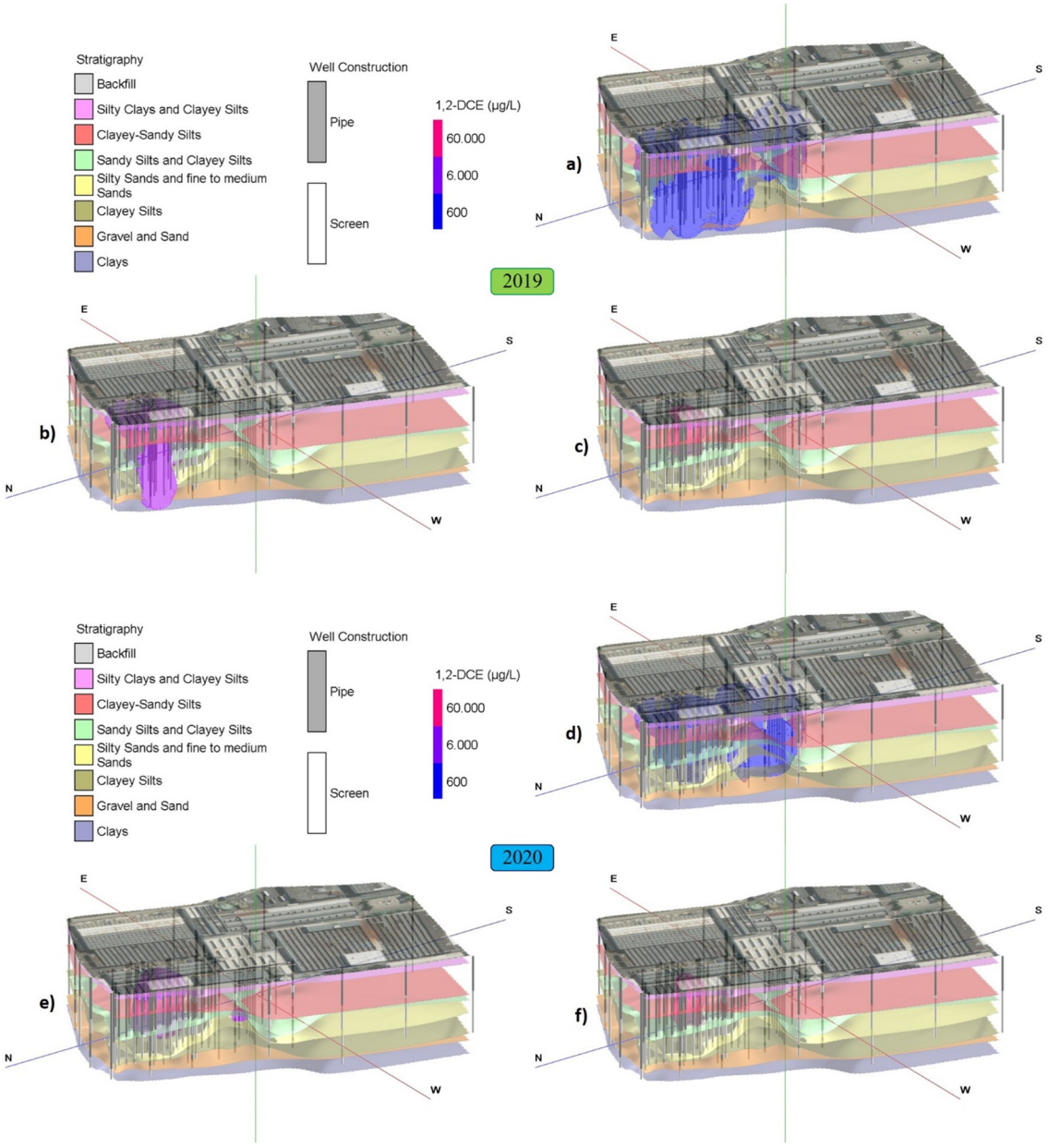

Fig. 4. Stratigraphic contacts, construction scheme of piezometers, and contamination plume at different concentrations of 1,2-DCE detected in the monitoring network in 2019 and 2020. Figures a, b, and c refer to isoconcentration isosurfaces of 600 μg/L, 6000 μg/L, and 60,000 μg/L, respectively detected in 2019. Figures d, e, and f are related to isoconcentration isosurfaces of 600 μg/L, 6000 μg/L, and 60,000 μg/L respectively measured in 2020.

Contaminant plume is reduced through the combined action of the IEG-GCW®s and the pumping wells within the site. The modification of the hydraulic configuration in 2020 results in the mobilization of aged contaminants, which are adsorbed to the fine matrix, at the recirculation well. The mobilizing action on adsorbed pollutants that is triggered by the 2020 reconfiguration can also be observed at MLWS5, detecting a plume with a concentration of 600 μg/L. Here, the interacting recirculation cells generated by different GCWs potentially lead to the mobilization of secondary contaminant sources. The release of pollutants, which are currently associated with fine-grained levels, is governed by the back-diffusion phenomenon and is accelerated by the recirculation well under conditions of low hydraulic disturbance.

In the NW sector of the site, where the DCS well and the perimeter hydraulic barrier are installed, the data-driven model delineates an area impacted by significant concentrations of contaminants not identified in previous studies. At the DCS system, the high concentrations of 1,2-DCE detected in the aquifer over time are consistent with the hypothesis of the presence of chlorinated solvents adsorbed to the fine solid matrix. This assumption is supported by evidence found at the site under investigation in the suit of previous studies (Ciampi et al., 2019b; Petrangeli Papini et al., 2016; Pierro et al., 2017), which identified secondary sources of residual-phase contamination. In the NW sector of the plant, boundary pumping wells may ensure the groundwater recall (as evidenced by Fig. 2) and hydraulic confinement, by preventing the migration of contaminants off-site.

Time trends of plume volumes at different isoconcentrations of VC provide interesting insights into the dynamics of contamination and decontamination in this geological scenario. Fig. 6 portrays groundwater quality status in 2014 and 2019, two key moments that are marked by the pilot-scale IEG-GCW® implementation and the remediation upscaling, respectively.

Confronting the figures related to 2014 and 2019 leads to intriguing hints on the mobilization mechanisms of secondary sources and the biodegradation processes in place. Fig. 6a and d unequivocally highlight the growth of the VC plume volume at 500 μg/L over time. Such an effect is most likely linked to an acceleration of contaminant desorption processes and/or to BRD enhancement induced by the realization of all recirculation systems in the central portion of the site. Besides, in the same area (the primary source of contamination), full-scale deployment entails a sudden depletion of the highest isoconcentration isosurface in the primary source area, which could be attributed to BRD and VC biodegradation.

Processing operations conducted on the 3D solid models yielded estimates of the volumes enclosed within each isosurface at different chlorinated solvent concentrations. Fig. 7a and b shows the time trends of the volumes at different isoconcentration obtained from interpolation of the monitoring data available for 1,2-DCE and VC. Analysis of Fig. 7a and b provides compelling insights regarding the dynamics of pollution and remediation of the site, depending on the actions undertaken over time. Tiny quantities of pollutants were withdrawn and/or mobilized

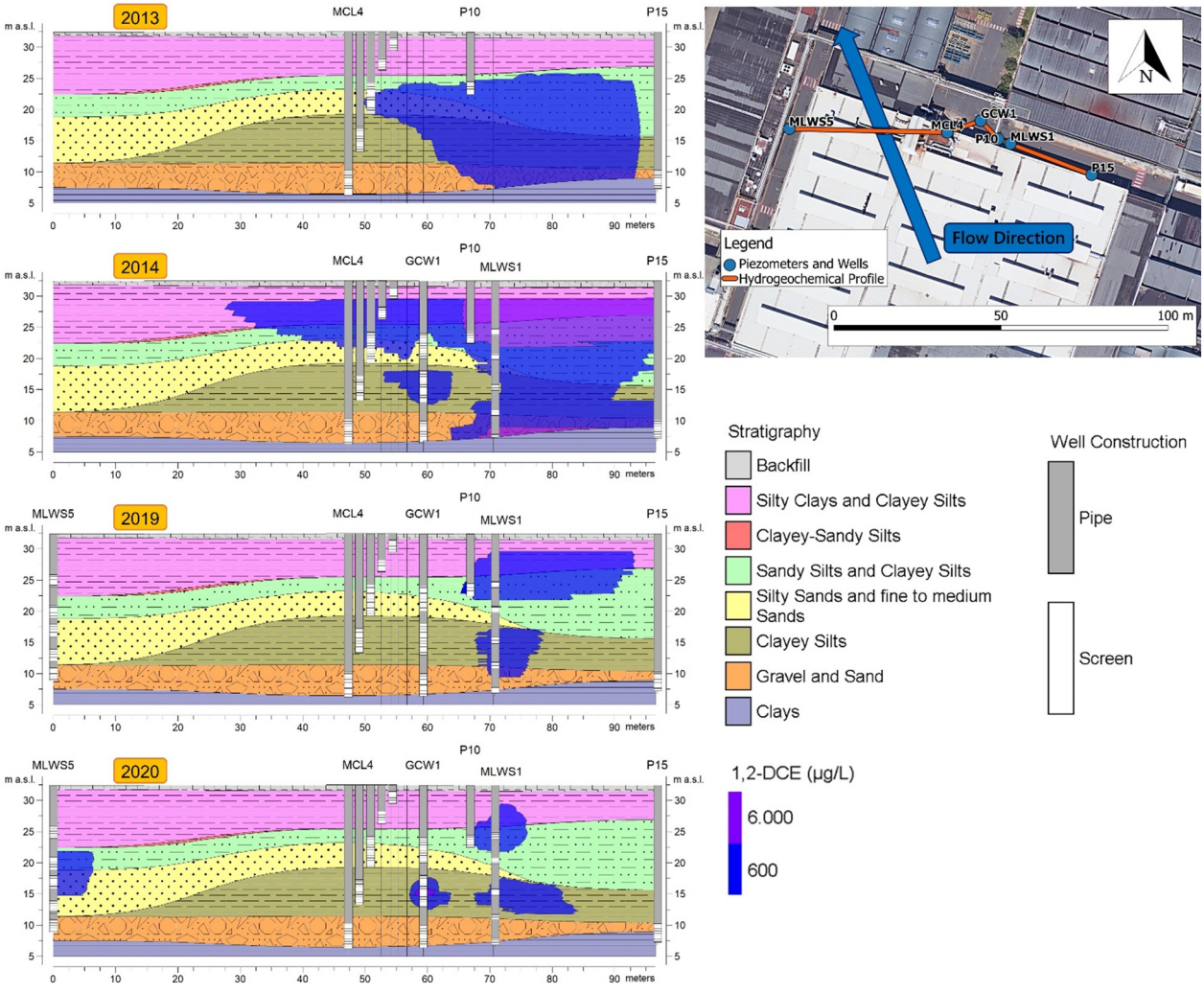

Fig. 5. Hydrogeochemical sections relating to concentrations of 1,2-DCE detected in groundwater sampling wells around the primary source area.

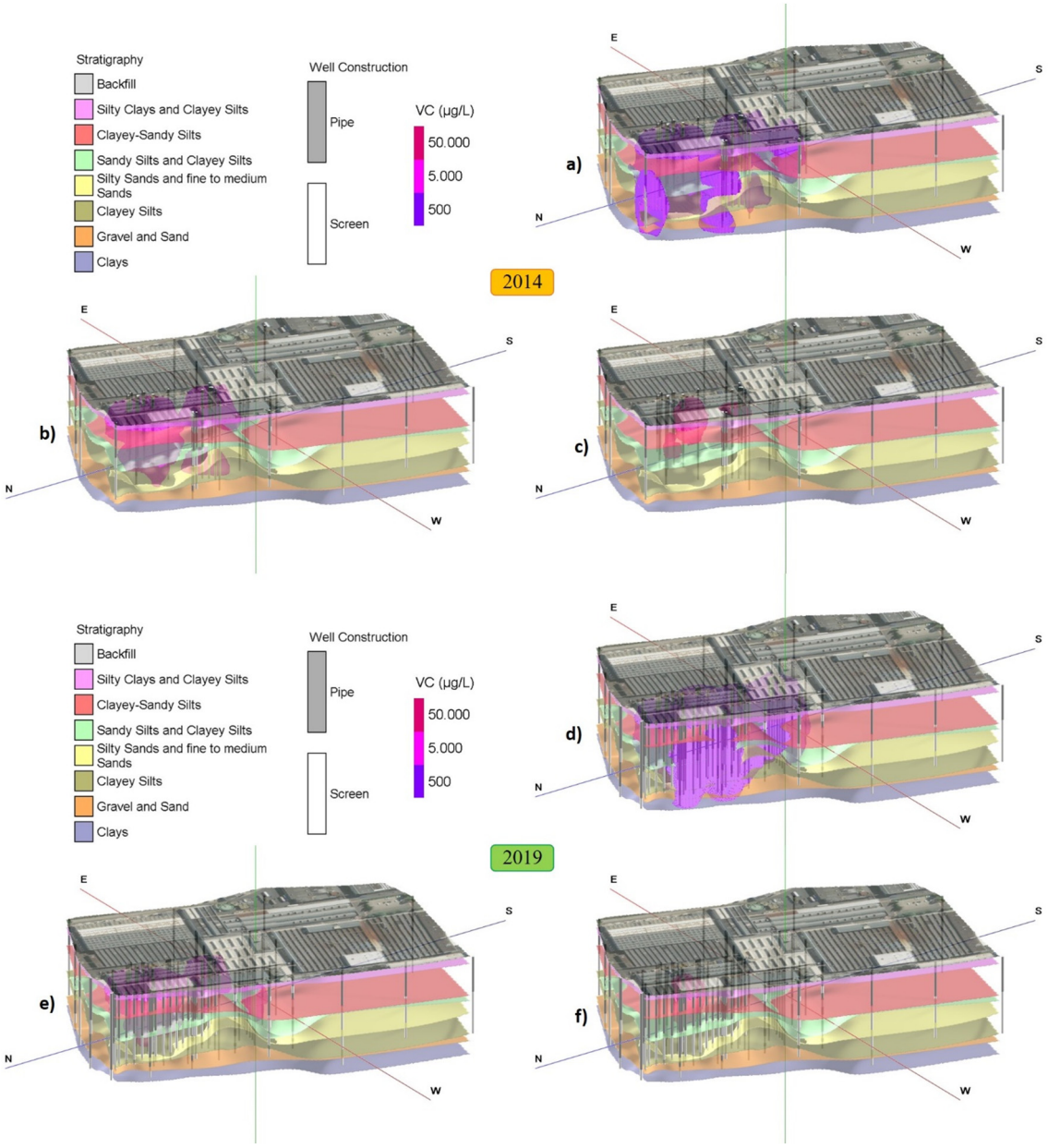

Fig. 6. Stratigraphic contacts, construction scheme of piezometers, and contamination plume at different concentrations of VC detected in the monitoring network in 2014 and 2019. Figures a, b, and c refer to isoconcentration isosurfaces of 500 µg/L, 5000 µg/L, and 50,000 µg/L, respectively detected in 2014. Figures d, e, and f are related to isoconcentration isosurfaces of 500 µg/L, 5000 µg/L, and 50,000 µg/L respectively measured in 2019.

although both pumping and boundary barrier wells were operating in 2013. Traditional extraction techniques notoriously have a limited influence on lower permeability layers where pollutants are adsorbed or in the residual phase (Brusseau and Guo, 2014; Petrangeli Papini et al., 2016; Tatti et al., 2019). On the other hand, since 2014, when the first IEG-GCW® was performed on the pilot scale, a growing potential to mobilize large amounts of pollutants from secondary sources of pollution has been manifest. In more detail, from 2013 to 2014, the graphs reported in Fig. 7a and b emphasize ascending trends reflecting the increase in the number of monitoring points over time, leading to the capture and discretization of real groundwater contamination with an increased resolution with the same volume analyzed. To this effect can be added the contribution resulting from the mobilization of contaminants adsorbed on the fine matrix, induced by the recirculation action of the IEG-GCW® well implemented at the pilot scale. Analyzing the data for 2014 (pilot test), 2019 (full-scale), and 2020 (change in pumping configuration), a consistent drop in groundwater volumes impacted by the presence of 1,2-DCE and VC appears, resulting in a reduction in the total mass of contaminant present at the site. Volumes calculated for the 500 µg/L VC isosurface deviate from this general trend, exhibiting a large increase in 2019 before decreasing again in 2020. This finding is associated with the enhanced dechlorinating activity resulting from the implementation of the full-scale intervention and the stimulation of biological reductive dechlorination by the electron donor (Matturro et al., 2018). This phenomenon could be more pronounced for isosurface plumes at low concentrations because of the augmented resolution detail of discretizing hydrochemical peculiarities, leading to a consequent improved ability to capture and explain decontamination mechanisms at the site scale. In contrast to what has been observed at other sites recording VC accumulation (Mayer-Blackwell et al., 2017; Sleep et al., 2005; Yu et al., 2018), the system compensates for the lack of an electron donor by supporting BRD reactions. Indeed, the last two years of monitoring evidenced a drastic drop in VC concentrations attributable to biological processes promoted by continuous

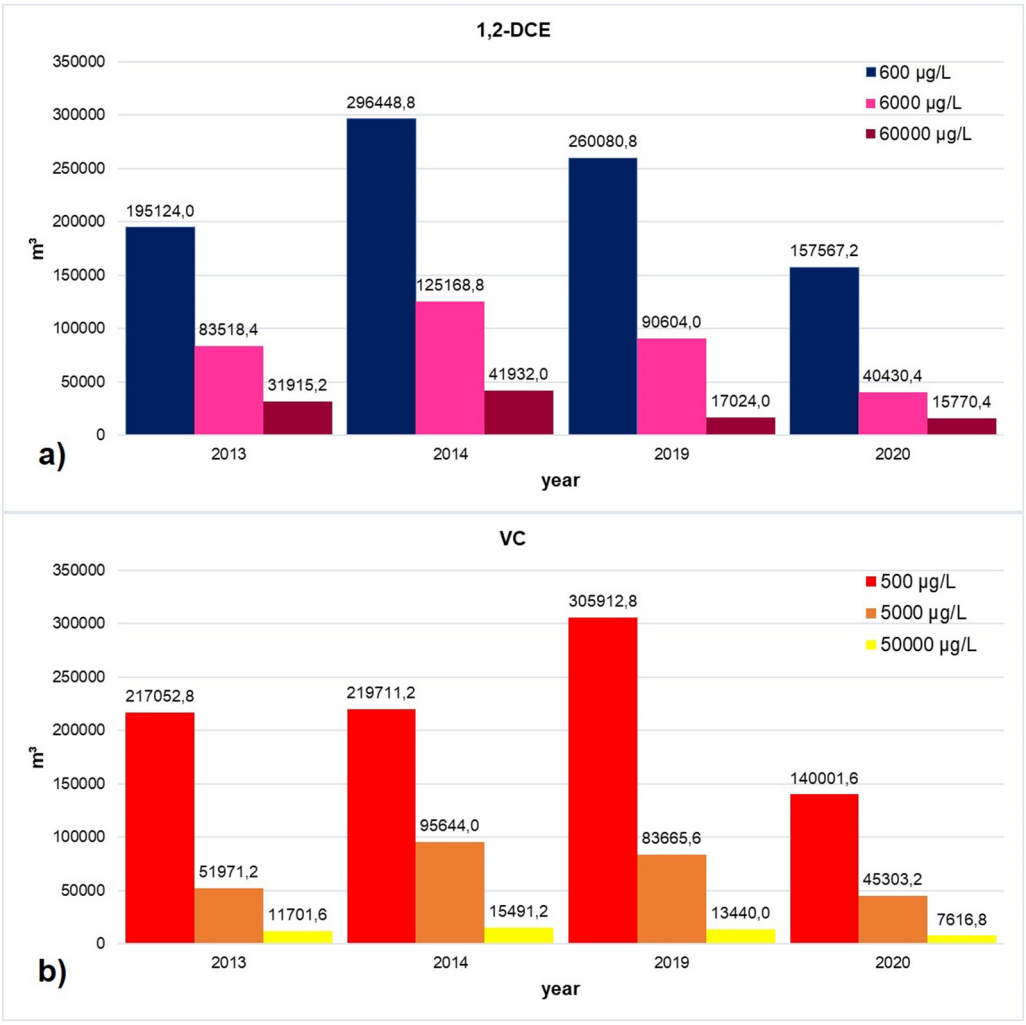

Fig. 7. Trend of plume volumes at different concentrations of 1,2-DCE (a) and VC (b) over time.

electron provision (Matturro et al., 2018). Also, Fig. 7a and b illuminates the effectiveness of adjusting the configuration of the remediation strategy adopted in the last two monitored years, with the same number of sampling points, in terms of its abatement capacity for dissolved organohalogenated compounds in groundwater.

3.2. Performance of IEG-GCW® treatment

The full-scale intervention reveals a clear pollutant mobilization impact generated by the recirculating system. The GCW2, designed for full-scale intervention, operates through the extraction of groundwater at the filter sections between 7 and 11 m (PNS1) and 15 and 19 m (PNS2) and its re-injection into the lower filter section between 22 and 26 m (PNS8), leading to the creation of recirculation cells. VC and 1,2-DCE concentrations in water pumped from the transmissive part (PNS2) approximate 70 µg/L, whereas chlorinated substance concentrations in water recovered from the low-permeability layer (PNS1) amount to about 4000 and 3000 µg/L for 1,2-DCE and VC, respectively. The chlorinated solvent concentration in groundwater recovered from the low permeability layer (PNS1) is much greater than that detected at monitoring point PNS2 (Fig. 8).

The above denotes that low-permeability horizons behave as adsorption and trapping zones for residual phase pollutants, classically unaffected by conventional extraction systems. Comparison of masses extracted per unit time from GCW1 (pilot test) and the entire pumping well system within the plant exemplifies the technology's performance in removing target contaminants (Table 1 of Supplementary Material). Under the same geologic setting and contaminant characteristics, a single GCW removed 60% of 1,2-DCE and 27% of VC (per unit of time) in comparison with the 13 pumping wells. The largest contribution, in terms of removed mass, is provided by the pump located at a low permeability level (PNS2). Although the PNS2 pump flow rate is 3% of the overall flow rate of the pumping wells, GCW1 removed 52% of 1,2-DCE and 22% of VC (per unit of time) in comparison with 13 pumping wells at the low permeability layer only. All these findings attest to the success of the adopted intervention in removing chlorinated solvents and mobilizing adsorbed pollutants in the residual phase, as well as to the sustainability and performance of the technology when compared with traditional physical extraction systems.

4. Discussion

In analogy to Curtis et al. (2019) and Trabelsi et al. (2013), knowledge-based geodatabase and data-driven modeling catch geological and hydrochemical conceptualization. Our massive hydrogeochemical framework further advances the utility of fused data sources and simplifies the process of data exchange to understand the relationships between underlying processes (Kueper et al., 2014). Knowledge extraction from geospatial data follows the concepts of Breunig et al. (2020), to bridge the gap between geo-computing with geospatial data management and to boost multi-modality information interoperability, positing a solution that guides end-process strategies. Merging diverse data

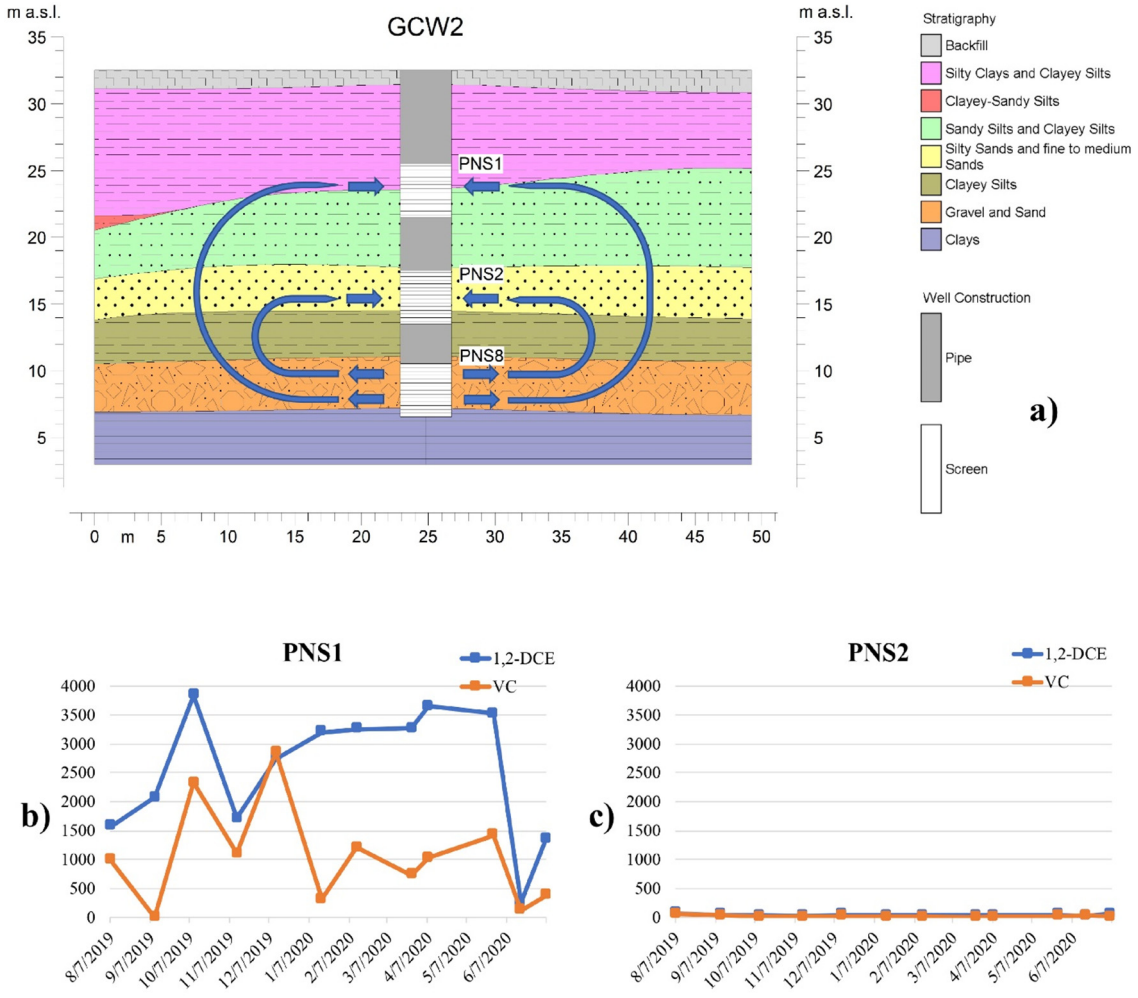

Fig. 8. Design scheme and configuration of the recirculation cells developed by GCW2, developed for the full-scale intervention (a). Trend of VC and cis-DCE concentrations in groundwater extracted from the low permeability zone (PNS1) (b) and the permeable zone (PNS2) (c).

sources into the data-driven model is crucial for the comprehension of the underlying mechanisms that affect the dynamics of contamination and decontamination at the site as a function of multiple ongoing remediation actions (Ciampi et al., 2021) and for quantifying the performance of the adopted remediation technology (Ciampi et al., 2019a). Such multi-source data rendering modality hints at the potential impact of hydraulic interference triggered by conventional extraction wells on GCWs. Remodulating and reducing the flow rates of some active wells within the influence radius of GCWs resonates in the mobilization of secondary contamination sources and potentially plays a key role in enhancing the effectiveness and performance of recirculating wells. According to Miller and Elmore (2005), the presence of pumping wells within the influence radius of GCW inevitably interferes with recirculation cells. Thus, the cone of depression induced by conventional pumping could be expected to distort the recirculation cells (Xia et al., 2019). Case studies on the hydrodynamic interaction of GCWs and conventional extraction wells are currently lacking. Hydrogeological numerical flow, transport modeling, and particle tracking method may explain both the interaction of GCWs with conventional extraction wells and the potential synergistic effect in pollutant mobilization induced by overlapping radii of influence of multiple recirculation wells (Johnson and Simon, 2007; Miller and Elmore, 2005; Zhu et al., 2020). Our hydrogeochemical model directs near real-time treatment reconfiguration and assesses the performance of innovative technology implemented for the first time on a large scale. The digital memory (Breunig et al., 2020) poses a platform for data sharing, data extraction and delivers a comprehensive and clear picture of environmental issues, following the evolution of contamination dynamics and remediation efforts (Ciampi et al., 2019a). This representation and calculation modality supports the hypothesis, largely demonstrated during the experiments conducted in the past, that the residual mass of contaminants is now associated with the zones of lower permeability (Ciampi et al., 2019b; Pierro et al., 2017; Petrangeli Papini et al., 2016), due to the significant heterogeneity of the saturated zone and the chemical and physical characteristics of the compounds leached into the subsoil (DNAPLs). Owing to slow molecular diffusion phenomena, low permeability lenses have become loaded with pollutants over time (Tatti et al., 2019). Once the contaminant has been exhausted in the more permeable portions, the lower permeability zones now release the contaminant by back-diffusion, a slow but continuous phenomenon that justifies the presence of such significant residual concentrations both in the monitoring piezometers and in the extraction systems controlling the groundwater. Also, Ciampi et al. (2019b) show that low-grade chlorinated products (i.e., 1,2-DCE and VC) are significantly prevalent than higher-grade chlorinated compounds (i.e., PCE and TCE). From 2008 to 2020, the average concentrations of PCE and TCE detected in groundwater vary between 0 and a few hundred μg/L. On the other hand, average values of DCE and VC concentrations over the same monitoring period range from several thousand to tens of thousands of μg/L (Fig. 1 of Supplementary Material). Cross-referencing this information with

microbiological characterization studies (Petrangeli Papini et al., 2016; Pierro et al., 2017) and with results of previous experiments of microcosm tests (Aulenta et al., 2007a), it is also possible to state that in these low-permeability zones, natural biological phenomena of reductive dechlorination have almost quantitatively transformed the initially spilled solvents into 1,2-DCE and VC. The findings of the microcosm study by Aulenta et al. (2005), Petrangeli Papini et al. (2016), and Pierro et al. (2017) demonstrate the potential to enhance complete dechlorination through the appropriate addition of an electron donor and/or through bioaugmentation. The above studies reveal that the lack of electron donors limits reductive dechlorination. Microbiological characterizations conducted by Matturro et al. (2018) and Pierro et al. (2017) prove that the slow release of electron donors modifies the groundwater microbiome with significant stimulation of autochthonous and specialized organohalide-respiring bacteria growth. In this scenario, characterized by an advanced stage of the reductive dechlorination process towards molecules with a reduced number of chloroatoms and a low rate of reductive dechlorination due to the exclusive presence of daughter products (i.e., DCE and VC) (Stroo and Ward, 2010; Tiehm and Schmidt, 2011), the lack of electron donor could not allow the completion of the dechlorination pathway with the accumulation of low-chlorinated compounds (Mayer-Blackwell et al., 2017; Sleep et al., 2005; Yu et al., 2018). The remediation plant associated with IEG-GCW®s, described by Ciampi et al. (2019b), Pierro et al. (2017), and Petrangeli Papini et al. (2016) is equipped with a system which can continuously supply electron donor, concluding the in situ biological reductive dechlorination process with the formation of ethane (Aulenta et al., 2007a; Aulenta et al., 2007b; Matturro et al., 2018; Ebrahimbabaie and Pichtel, 2021; Walaszek et al., 2021). The findings prove a contraction of VC plume volumes, evidently linked to the biodegradation of vinyl chloride by biological activity, largely supporting this claim.

5. Conclusions

The geodatabase governs all phases of remediation, from characterization refinement, through the selection of an operational strategy and the upscaling of its application. The data-driven 3D model contextualizes pollution dynamics and decontamination mechanisms within the geologic framework, as a function of hydraulic stresses and biological processes and in relation to remediation strategies enacted through time. Spatio-temporal data integration affords a qualitative and quantitative overview of the performance of the first full-scale approach, along with the opportunity to adapt and modify the intervention configuration based on the experimental results acquired in near real-time. The technological efficacy of IEG-GCW®s to reduce the mass of contaminant present in the residual phase and adsorbed to the low-permeability solid matrix has also been demonstrated, by monitoring the performance of the application of this innovative groundwater remediation strategy through hydrochemical modeling. Recirculation systems directly target secondary sources, accelerating the mobilization of pollutants while simultaneously the IEG-GCW®s-associated electron donor system promotes ISB and BRD pathway completion. The joint-modeling findings hint at the necessity to thoroughly investigate the hydraulic interactions generated due to well drawdown and recirculation cell development induced by IEG-GCW®s, which could potentially trigger a modification of groundwater flow vectors. This issue can dramatically affect the mobilization processes of old and residual phase contaminants and is of crucial importance in complex contaminated sites experiencing multiple groundwater remediation techniques.

CRediT authorship contribution statement

Paolo Ciampi: Writing – original draft, Software, Conceptualization, Data curation. **Carlo Esposito:** Methodology, Visualization, Supervision. **Ernst Bartsch:** Investigation, Data curation, Writing – review & editing. **Eduard J. Alesi:** Validation, Supervision, Writing – review & editing. **Marco Petrangeli Papini:** Conceptualization, Project administration, Methodology, Supervision.

Declaration of competing interest

The authors declare that they have no known competing financial interests or personal relationships that could have appeared to influence the work reported in this paper.

Acknowledgments

We thank the reviewers for their comments that helped to improve the quality of this manuscript.

Appendix A. Supplementary data

Supplementary data to this article can be found online at https://doi.org/10.1016/j.scitotenv.2021.148649.

References

Arlotti, D., Bozzini, R., Petitta, M., Mancini, M., Pianu, M., Alberto Blanco, G., Sbarbati, C., Colombo, R., 2012. Control and dynamic management of a sixty-seven wells hydraulic barrier. Chem. Eng. Trans. 28, 247–252. https://doi.org/10.3303/CET1228042.

Aulenta, F., Majone, M., Verbo, P., Tandoi, V., 2002. Complete dechlorination of tetrachloroethene to ethene in presence of methanogenesis and acetogenesis by an anaerobic sediment microcosm. Biodegradation. 13, 411–424. https://doi.org/10.1023/A:1022868712613.

Aulenta, F., Bianchi, A., Majone, M., Petrangeli Papini, M., Potalivo, M., Tandoi, V., 2005. Assessment of natural or enhanced in situ bioremediation at a chlorinated solvent contaminated aquifer in Italy: a microcosm study. Environ. Int. 31, 185–190. https://doi.org/10.1016/j.envint.2004.09.014.

Aulenta, F., Pera, A., Rossetti, S., Petrangeli Papini, M., Majone, M., 2007a. Relevance of side reactions in anaerobic reductive dechlorination microcosms amended with different electron donors. Water Res. 41 (1), 27–38. https://doi.org/10.1016/j.watres.2006.09.019.

Aulenta, F., Catervi, A., Majone, M., Panero, S., Reale, P., Rossetti, S., 2007b. Electron transfer from a solid-state electrode assisted by methyl viologen sustains efficient microbial reductive dechlorination of TCE. Environ. Sci. Technol. 41 (7), 2554–2559. https://doi.org/10.1021/es0624321.

Azzellino, A., Colombo, L., Lombi, S., Marchesi, V., Piana, A., Merri, A., Alberti, L., 2019. Groundwater diffuse pollution in functional urban areas: the need to define anthropogenic diffuse pollution background levels. Sci. Total Environ. 656, 1207–1222. https://doi.org/10.1016/j.scitotenv.2018.11.416.

Barbosa, S., Almeida, J., Chambel, A., 2019. A geostatistical methodology to simulate the transmissivity in a highly heterogeneous rock body based on borehole data and pumping tests. Hydrogeol. J. 27, 1969–1998. https://doi.org/10.1007/s10040-019-01980-7.

Borden, R.C., Richardson, S.D., Bodour, A.A., 2019. Enhanced reductive dechlorination of trichloroethene in an acidic DNAPL impacted aquifer. J. Environ. Manag. 237, 617–628. https://doi.org/10.1016/j.jenvman.2018.12.093.

Breunig, M., Bradley, P.E., Jahn, M., Kuper, P., Mazroob, N., Rösch, N., Al-Doori, M., Stefanakis, E., Jadidi, M., 2020. Geospatial data management research: progress and future directions. ISPRS Int. J. Geo Inf. 9 (2), 95. https://doi.org/10.3390/ijgi9020095.

Brooks, M.C., Yarney, E., Huang, J., 2021. Strategies for managing risk due to back diffusion. Groundw. Monit. R. 41, 76–98. https://doi.org/10.1111/gwmr.12423.

Brusseau, M.L., Guo, Z., 2014. Assessing contaminant-removal conditions and plume persistence through analysis of data from long-term pump-and-treat operations. J. Contam. Hydrol. 164, 16–24. https://doi.org/10.1016/j.jconhyd.2014.05.004.

Carey, G.R., McBean, E.A., Feenstra, S., 2014. DNAPL source depletion: 2. Attainable goals and cost–benefit analyses. Remediation. 24, 79–106. https://doi.org/10.1002/rem.21406.

Ciampi, P., Esposito, C., Viotti, P., Boaga, J., Cassiani, G., Petrangeli Papini, M., 2019a. An integrated approach supporting remediation of an aquifer contaminated with chlorinated solvents by a combination of adsorption and biodegradation. Appl. Sci. 9 (20), 4318. https://doi.org/10.3390/app9204318.

Ciampi, P., Esposito, C., Cassiani, G., Deidda, G.P., Rizzetto, P., Petrangeli Papini, M., 2021. A field-scale remediation of residual light non-aqueous phase liquid (LNAPL): chemical enhancers for pump and treat. Environ. Sci. Pollut. Res. https://doi.org/10.1007/s11356-021-14558-2.

Ciampi, P., Esposito, C., Petrangeli Papini, M., 2019b. Hydrogeochemical model supporting the remediation strategy of a highly contaminated industrial site. Water. 11 (7), 1371. https://doi.org/10.3390/w11071371.

Colombano, S., Davarzani, H., Van Hullebusch, E.D., Huguenot, D., Guyonnet, D., Deparis, J., Lion, F., Ignatiadis, I., 2021. Comparison of thermal and chemical enhanced recovery of DNAPL in saturated porous media: 2D tank pumping experiments and two-phase flow modelling. Sci. Total Environ. 760, 143958. https://doi.org/10.1016/j.scitotenv.2020.143958.

Cormier, S.M., Suter, G.W., 2008. A framework for fully integrating environmental assessment. Environ. Manag. 42, 543–556. https://doi.org/10.1007/s00267-008-9138-y.

Curtis, Z.K., Liao, H., Li, S.G., Sampath, P.V., Lusch, D.P., 2019. A multiscale assessment of shallow groundwater salinization in Michigan. Groundwater. 57, 784–806. https://doi.org/10.1111/gwat.12873.
Dai, C., Zhou, Y., Peng, H., Huang, S., Qin, P., Zhang, J., Yang, Y., Luo, L., Zhang, X., 2018. Current progress in remediation of chlorinated volatile organic compounds: a review. J. Ind. Eng. Chem. 62, 106–119. https://doi.org/10.1016/j.jiec.2017.12.049.
Davis, D., Miller, O.J., 2018. Addition of divalent iron to electron donor mixtures for remediation of chlorinated ethenes: a study of 100 wells. Remediation. 29, 37–44. https://doi.org/10.1002/rem.21581.
Day-Lewis, F.D., Slater, L.D., Robinson, J., Johnson, C.D., Terry, N., Werkema, D., 2017. An overview of geophysical technologies appropriate for characterization and monitoring at fractured-rock sites. J. Environ. Manag. 204 (2), 709–720. https://doi.org/10.1016/j.jenvman.2017.04.033.
Dinkel, E., Braun, B., Schröder, J., Muhrbeck, M., Reul, W., Meeder, A., Szewzyk, U., Scheytt, T., 2020. Groundwater circulation wells for geothermal use and their impact on groundwater quality. Geothermics. 86. https://doi.org/10.1016/j.geothermics.2020.101812.
Douglas, J., Mateas, D.J., Geoffrey, R., Tick, G.R., Kenneth, C., Carroll, K.C., 2017. In situ stabilization of NAPL contaminant source-zones as a remediation technique to reduce mass discharge and flux to groundwater. J. Contam. Hydrol. 204, 40–56. https://doi.org/10.1016/j.jconhyd.2017.07.007.
Ebrahimbabaie, P., Pichtel, J., 2021. Biotechnology and nanotechnology for remediation of chlorinated volatile organic compounds: current perspectives. Environ. Sci. Pollut. Res. 28, 7710–7741. https://doi.org/10.1007/s11356-020-11598-y.
Engelmann, C., Schmidt, L., Werth, C.J., Walther, M., 2019. Quantification of uncertainties from image processing and analysis in laboratory-scale DNAPL release studies evaluated by reflective optical imaging. Water. 11 (11), 2274. https://doi.org/10.3390/w1111227.
Filippini, M., Nijenhuis, I., Kümmel, S., Chiarini, V., Crosta, G., Richnow, H.H., Gargini, A., 2018. Multi-element compound specific stable isotope analysis of chlorinated aliphatic contaminants derived from chlorinated pitches. Sci. Total Environ. 640–641, 153–162. https://doi.org/10.1016/j.scitotenv.2018.05.285.
Guerra, V., Guerra, C., Nesci, O., 2020. Geomorphology of the town of Rimini and surrounding areas (Emilia-Romagna, Italy). J. Maps. https://doi.org/10.1080/17445647.2020.1800527.
Heron, G., Bierschenk, J., Swift, R., Watson, R., Kominek, M., 2016. Thermal DNAPL source zone treatment impact on a CVOC plume. Groundw. Monit. R. 36, 26–37. https://doi.org/10.1111/gwmr.12148.
Herrling, B., Stamm, J., Buermann, W., 1991a. Hydraulic circulation system for in situ bioreclamation and/or in situ remediation of strippable contamination. In: Hinchee, R.E., Olfenbuttel, R.F. (Eds.), In Situ Bioreclamation. Butterworth-Heinemann, Boston, MA, USA, pp. 173–195.
Herrling, B., Stamm, J., Alesi, E.J., Brinnel, P., Hirschberger, F., Sick, M.R., 1991b. In situ groundwater remediation of strippable contaminants by vacuum vaporizer wells (UVB): operation of the well and report about cleaned industrial sites. Proceedings, Third Forum on Innovative Hazardous Waste Treatment Technologies: Domestic and International. Dallas, TX, USA, June 11–13. EPA/540/2-91/016, pp. 1–13.
Johnson, R.J., Simon, M.A., 2007. Evaluation of groundwater flow patterns around a dual-screened groundwater circulation well. J. Contam. Hydrol. 93 (1–4), 188–202. https://doi.org/10.1016/j.jconhyd.2007.02.003.
Koch, J., Nowak, W., 2015. Predicting DNAPL mass discharge and contaminated site longevity probabilities: conceptual model and high-resolution stochastic simulation. Water Resour. Res. 51, 806–831. https://doi.org/10.1002/2014WR015478.
Kueper, B.H., Stroo, H.F., Vogel, C.M., Ward, C.H., 2014. Chlorinated Solvent Source Zone Remediation. Springer, New York https://doi.org/10.1007/978-1-4614-6922-3.
Langwaldt, J.H., Puhakka, J.A., 2000. On-site biological remediation of contaminated groundwater: a review. Environ. Pollut. 107 (2), 187–197. https://doi.org/10.1016/S0269-7491(99)00137-2.
Lee, I., Bae, J., McCarty, P.L., 2007. Comparison between acetate and hydrogen as electron donors and implications for the reductive dehalogenation of PCE and TCE. J. Contam. Hydrol. 94 (1–2), 76–85. https://doi.org/10.1016/j.jconhyd.2007.05.003.
Litvinenko, A., Logashenko, D., Tempone, R., Wittum, G., Keyes, D., 2020. Solution of the 3D density-driven groundwater flow problem with uncertain porosity and permeability. Int. J. Geomath. 11, 10. https://doi.org/10.1007/s13137-020-0147-1.
Liu, C., Tseng, D., Wang, C., 2006. Effects of ferrous ions on the reductive dechlorination of trichloroethylene by zero-valent iron. J. Hazard. Mater. 136 (3), 706–713. https://doi.org/10.1016/j.jhazmat.2005.12.045.
Mackay, D.M., Roberts, P.V., Cherry, J.A., 1985. Transport of organic contaminants in groundwater. Distribution and fate of chemicals in sand and gravel aquifers. Environ. Sci. Technol. 19, 384–392. https://doi.org/10.1021/es00135a001.
Maples, S.R., Fogg, G.E., Maxwell, R.M., 2019. Modeling managed aquifer recharge processes in a highly heterogeneous, semi-confined aquifer system. Hydrogeol. J. 27, 2869–2888. https://doi.org/10.1007/s10040-019-02033-9.
Matturro, B., Pierro, L., Frascadore, E., Petrangeli Papini, M., Rossetti, S., 2018. Microbial community changes in a chlorinated solvents polluted aquifer over the field scale treatment with poly-3-hydroxybutyrate as amendment. Front. Microbiol. 9, 1664. https://doi.org/10.3389/fmicb.2018.01664.
Mayer-Blackwell, K., Azizian, M.F., Green, J.K., Spormann, A.M., Semprini, L., 2017. Survival of vinyl chloride respiring Dehalococcoides mccartyi under long-term electron donor limitation. Environ. Sci. Technol. 38 (4), 1102–1107. https://doi.org/10.1021/acs.est.6b05050.
Mayo, A.L., 2010. Ambient well-bore mixing, aquifer cross-contamination, pumping stress, and water quality from long-screened wells: what is sampled and what is not? Hydrogeol. J. 18, 823–837. https://doi.org/10.1007/s10040-009-0568-2.
Miller, G.R., Elmore, A.C., 2005. Modeling of a groundwater circulation well removal action alternative. Pract. Period. Hazard. Toxic Radioact. Waste Manage. 9, 122–129. https://doi.org/10.1061/~ASCE!1090-025X~2005!9:2~122!.
Moeck, C., Radny, D., Popp, A., Brennwald, M., Stoll, S., Auckenthaler, A., Berg, M., Schirmer, M., 2017. Characterization of a managed aquifer recharge system using multiple tracers. Sci. Total Environ. 609, 701–714. https://doi.org/10.1016/j.scitotenv.2017.07.211.
Newell, C.J., Cowie, I., McGuire, T.M., McNab, W.W., 2006. Multiyear temporal changes in chlorinated solvent concentrations at 23 monitored natural attenuation sites. J. Environ. Eng. 132 (6), 653–663. https://doi.org/10.1061/(ASCE)0733-9372(2006)132:6(653).
Nsir, K., Schäfer, G., Di Chiara Roupert, R., Mercury, L., 2018. Pore scale modelling of DNAPL migration in a water-saturated porous medium. J. Contam. Hydrol. 215, 39–50. https://doi.org/10.1016/j.jconhyd.2018.07.001.
Orozco, A.F., Ciampi, P., Katona, T., Censini, M., Petrangeli Papini, M., Deidda, G.P., Cassiani, G., 2021. Delineation of hydrocarbon contaminants with multi-frequency complex conductivity imaging. Sci. Total Environ. 768. https://doi.org/10.1016/j.scitotenv.2021.144997.
Ouyang, Q., Lu, W., Miao, T., Deng, W., Jiang, C., Luo, J., 2017. Application of ensemble surrogates and adaptive sequential sampling to optimal groundwater remediation design at DNAPLs-contaminated sites. J. Contam. Hydrol. 207, 31–38. https://doi.org/10.1016/j.jconhyd.2017.10.007.
Petrangeli Papini, M., Majone, M., Arjmand, F., Silvestri, D., Sagliaschi, M., Sucato, S., Alesi, E., 2016. First pilot test on integration of GCW (groundwater circulation well) with ena (enhanced natural attenuation) for chlorinated solvents source remediation. Chem. Eng. Trans. 49, 91–96. https://doi.org/10.3303/CET1649016.
Pierro, L., Matturro, B., Rossetti, S., Sagliaschi, M., Sucato, S., Alesi, E., Bartsch, E., Arjmand, F., Petrangeli Papini, M., 2017. Polyhydroxyalkanoate as a slow-release carbon source for in situ bioremediation of contaminated aquifers: from laboratory investigation to pilot-scale testing in the field. New Biotechnol. 37, 60–68. https://doi.org/10.1016/j.nbt.2016.11.004.
Puigserver, D., Herrero, J., Parker, B.L., Carmona, J.M., 2020. Natural attenuation of pools and plumes of carbon tetrachloride and chloroform in the transition zone to bottom aquitards and the microorganisms involved in their degradation. Sci. Total Environ. 712, 135679. https://doi.org/10.1016/j.scitotenv.2019.135679.
Sleep, B.E., Brown, A.J., Lollar, B.S., 2005. Long-term tetrachlorethene degradation sustained by endogenous cell decay. J. Environ. Eng. Sci. 4 (1), 11–17. https://doi.org/10.1139/s04-038.
Steelman, C.M., Meyer, J.R., Wanner, P., Swanson, B.J., Conway-White, O., Parker, B.L., 2020. The importance of transects for characterizing aged organic contaminant plumes in groundwater. J. Contam. Hydrol. 235, 103728. https://doi.org/10.1016/j.jconhyd.2020.103728.
Stroo, H., Ward, H., 2010. In Situ Remediation of Chlorinated Solvent Plumes. Springer, New York https://doi.org/10.1007/978-1-4419-1401-9.
Tatti, F., Petrangeli Papini, M., Torretta, V., Mancini, G., Boni, M.R., Viotti, P., 2019. Experimental and numerical evaluation of Groundwater Circulation Wells as a remediation technology for persistent, low permeability contaminant source zones. J. Contam. Hydrol. 222, 89–100. https://doi.org/10.1016/j.jconhyd.2019.03.001.
Tiehm, A., Schmidt, K.R., 2011. Sequential anaerobic/aerobic biodegradation of chloroethenes—aspects of field application. Curr. Opin. Biotechnol. 22 (3), 415–421. https://doi.org/10.1016/j.copbio.2011.02.003.
Trabelsi, F., Tarhouni, J., Mammou, A.B., Ranieri, G., 2013. GIS-based subsurface databases and 3-D geological modeling as a tool for the set up of hydrogeological framework: Nabeul–Hammamet coastal aquifer case study (Northeast Tunisia). Environ. Earth Sci. 70, 2087–2105. https://doi.org/10.1007/s12665-011-1416-y.
Tseng, H., Su, J., Liang, C., 2011. Synthesis of granular activated carbon/zero valent iron composites for simultaneous adsorption/dechlorination of trichloroethylene. J. Hazard. Mater. 192 (2), 500–506. https://doi.org/10.1016/j.jhazmat.2011.05.047.
Walaszek, M., Cary, L., Billon, G., Blessing, M., Bouvet-Swialkowski, A., George, M., Criquet, J., Mossmann, J.R., 2021. Dynamics of chlorinated aliphatic hydrocarbons in the chalk aquifer of northern France. Sci. Total Environ. 757, 143742. https://doi.org/10.1016/j.scitotenv.2020.143742.
Wu, J., Li, P., Qian, H., 2015. Hydrochemical characterization of drinking groundwater with special reference to fluoride in an arid area of China and the control of aquifer leakage on its concentrations. Environ. Earth Sci. 73, 8575–8588. https://doi.org/10.1007/s12665-015-4018-2.
Xia, Q., Zhang, Q., Xu, M., Tang, Y., Teng, H., 2019. Visualizing hydraulic zones of a vertical circulation well in presence of ambient flow. Desalin. Water Treat. 159, 151–160. https://doi.org/10.5004/dwt.2019.24098.
Yang, L., Wang, X., Mendoza-Sanchez, I., Abriola, L.M., 2018. Modeling the influence of coupled mass transfer processes on mass flux downgradient of heterogeneous DNAPL source zones. J. Contam. Hydrol. 211, 1–14. https://doi.org/10.1016/j.jconhyd.2018.02.003.
Yu, R., Andrachek, R.G., Lehmicke, L.G., Freedman, D.L., 2018. Remediation of chlorinated ethenes in fractured sandstone by natural and enhanced biotic and abiotic processes: a crushed rock microcosm study. Sci. Total Environ. 626, 497–506. https://doi.org/10.1016/j.scitotenv.2018.01.064.
Zhu, L., Li, M., Li, C., Shang, J., Chen, G., Zhang, B., Wang, X., 2013. Coupled modeling between geological structure fields and property parameter fields in 3D engineering geological space. Eng. Geol. 167, 105–116. https://doi.org/10.1016/j.enggeo.2013.10.016.
Zhu, Q., Wen, Z., Zhan, H., Yuan, S., 2020. Optimization strategies for in situ groundwater remediation by a vertical circulation well based on particle-tracking and node-dependent finite difference methods. Water Resour. Res. 56, e2020WR027396. https://doi.org/10.1029/2020WR027396.
Zume, J., Tarhule, A., 2008. Simulating the impacts of groundwater pumping on stream-aquifer dynamics in semiarid northwestern Oklahoma, USA. Hydrogeol. J. 16, 797–810. https://doi.org/10.1007/s10040-007-0268-8.